Structure and Desorption Energetics of Ultrathin D_2O Ice Overlayers on Serine- and Serinephosphate-Terminated Self-Assembled Monolayers

Mattias Östblom,[†] Johan Ekeroth,[‡] Peter Konradsson,[‡] and Bo Liedberg*[,†]

Divisions of Molecular Physics and Organic Chemistry, Department of Physics, Chemistry, and Biology, Linköping University, SE-581 83 Linköping, Sweden

Received: September 13, 2005; In Final Form: November 29, 2005

This paper reports on the structure and desorption dynamics of thin D_2O ice overlayers (0.2−10 monolayers) deposited on serine- and serinephosphate- (with H^+, Na^+, Ca^{2+} counterions) terminated self-assembled monolayers (SAMs). The D_2O ice overlayers are deposited on the SAMs at ∼85 K in ultrahigh vacuum and characterized with infrared reflection absorption spectroscopy (IRAS). Reflection absorption (RA) spectra obtained at sub-monolayer D_2O coverage reveal that surface modes, e.g. free dangling OD stretch, dominate on the serine SAM surface, whereas vibrational modes characteristic for bulk ice are more prominent on the serinephosphate SAMs. Temperature programmed desorption mass spectrometry (TPD-MS) and TPD-IRAS are subsequently used to investigate the energetics and the structural transitions occurring in the ice overlayer during temperature ramping. D_2O ice (∼2.5 monolayers) on the serine SAMs undergoes a gradual change from an amorphous- to a crystalline-like phase upon increasing the substrate temperature. This transition is not as pronounced on the serine phosphate SAM most likely because of reduced mobility due to strong pinning to the surface. We show also that the energy of desorption for a sub-monolayer of D_2O ice on serinephosphate SAM surfaces with a Na^+ and Ca^{2+} counterions is equally high or even exceeds previously reported values for analogous high-energy SAMs.

Introduction

Phosphates play a crucial role in biology, both in the form of energy-rich groups in molecules such as ATP, as a part of the backbone structure of DNA, as well as an important component in bone together with calcium. This particular material, calcium hydroxyapatite (HA), has been studied extensively within the biomaterials science community, because of its importance for the design and development of new implantable devices, joints, and prostheses. It is, for example, of interest to develop coating processes that can improve the adhesion and integration between the biomaterial and bone. A large number of studies of the mineralization processes of calcium phosphates including work in suspension[1−4] and on solid supports[5−7] have been published. Moreover, Küther et al.[8] utilized self-assembled monolayers to investigate the nucleation and growth of $CaCO_3$ crystals. We recently synthesized a range of organic phosphates for self-assembly on gold.[9] The purpose was to develop surface coating that could be used as a template for mineralization, e.g. of HA, and to produce a set of biomimetic surfaces for fundamental studies of reactions where phosphates are involved.[10,11]

We have for a long time been interested in the structure and properties of water, in particular, interfacial water. This type of water is analogous to the water present in hydration layers around ions and organic structures both in solution and at surfaces.[12−14] Interfacial water also plays an important role during mineralization,[15,16] and the structure of water close to HA, collagen, and a mixture thereof has been investigated.[17] The aim of the present study is to investigate interfacial water in the form of ultrathin ice overlayers on organic surfaces. Such studies have been undertaken before at our laboratory as well as by others.[18−24] The main emphasis is on the phase behavior and energetics of ice on surfaces that mimic the structure of HA. These surfaces have been prepared on gold using thiols with serine and serinephosphate tail groups,[9] Scheme 1. The ice overlayers are studied at low temperature (85−250 K) on the serine and serinephosphate (H^+, Na^+, and Ca^{2+}) SAMs using temperature programmed desorption infrared reflection spectroscopy (TPD-IRAS) and mass spectrometry (TPD-MS).

Experimental Section

Materials and Sample Preparation. The serine and serinephosphate derivatives were synthesized following recently published protocols.[9] The substrates used for incubation were 2000 Å thick electron-beam evaporated gold films on top of freshly cleaned and precut (100) silicon slides that were precoated with a 25 Å adhesive layer of titanium. All evaporations took place in a Balzers UMS 500 P system operating at a base pressure of $\sim 10^{-9}$ Torr and an evaporation pressure of $\sim 10^{-7}$ Torr. The evaporation rate was 10 Å s^{-1} for gold and 1 Å s^{-1} for titanium. Prior to incubation in the ethanol thiol solutions, the samples were thoroughly cleaned in a 5:1:1 mixture of distilled water:25% hydrogen peroxide:30% ammonia for 10 min at 80 °C. The samples were incubated for a minimum of 15 h in 1 mM ethanol solutions of the thiols. The samples were rinsed with ethanol after incubation, ultrasonicated in ethanol for 3 min to remove physisorbed thiols, rinsed in ethanol again, and finally blown dry in N_2. In some cases the H^+ counterion was replaced with a different counterion (Na^+, Ca^{2+}); this procedure is described elsewhere.[9] Before insertion in the introduction chamber of the ultrahigh-vacuum system was the

* Corresponding author. E-mail: bolie@ifm.liu.se. Phone: +46-13-281877. Fax: +46-13-288969.
† Division of Melecular Physics.
‡ Division of Organic Chemistry.

10.1021/jp055169j CCC: $33.50
Published on Web 01/06/2006

SCHEME 1: Molecules and Counterions Used for Creating the Self-Assembled Monolayer Substrates

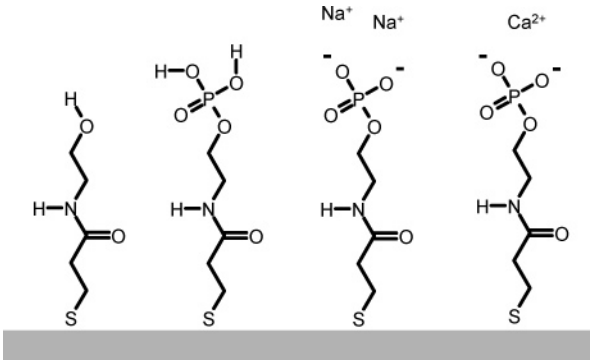

sample surface blown dry with nitrogen gas. The outcome of the self-assembly process in terms of monolayer thickness and wetting characteristics was immediately checked on twin samples using a Rudolph Research AutoELIII ellipsometer and a Ramé-Hart NRL 100 goniometer.

Ultrahigh-Vacuum System and TPD. The TPD-MS and temperature programmed desorption infrared reflection−absorption spectroscopy (TPD-IRAS) measurements were undertaken in a home-built ultrahigh-vacuum system described in detail elsewhere.[20] The base pressure in the measurement chamber was 5×10^{-10} Torr and in the preparation chamber 5×10^{-9} Torr. The TPD-MS traces were obtained with a Hiden HAL 301 positive ion counting quadropole analyzer mounted in front of the sample in the measurement chamber. The sample temperature (85−250 K) was monitored with a Pt 100 element and controlled with a Eurotherm controller/programmer, Type 818. Deuterated water (Merck) was deposited onto the sample surface at 85 K via a capillary tube facing the sample surface. The heating rate used in the TPD experiments was 0.33 K/s.

The infrared measurements were made with a Bruker IFS 22 spectrometer, aligned at an angle of incidence of 83° and equipped with a narrow band liquid nitrogen cooled MCT detector. The reflection absorption (RA) spectra were recorded at a spectral resolution of 2 cm^{-1}. A low noise background spectrum was always recorded at 85 K before each deposition of D_2O by averaging 500 interferograms (∼15 min acquisition time). After the D_2O deposition, but prior to the TPD-MS, another RA spectrum was recorded in order to determine the coverage and structure of the deposited D_2O ice overlayer at 85 K. A previously developed infrared method was used to calculate the equivalent thickness and coverage (monolayers) of the deposited D_2O ice overlayer.[21] A new RA spectrum was recorded every 20 s (20 scans/spectrum) during the TPD-MS scan. Thus, each RA spectrum represents approximately a 7 K interval. These dynamic measurements were performed to monitor the structural transitions occurring prior to and during the desorption event. The TPD-MS scan was terminated at ∼250 K for each measurement, after which the sample was cooled to 85 K, and a RA spectrum was recorded to check whether the surface was irreversibly affected by the adsorption/desorption of the D_2O ice layer. If the surface was unaffected, another measurement cycle was performed at another coverage using the same surface.

Results and Discussion

Structure of Deposited D_2O Ice. The D_2O molecule displays three normal modes of vibration—the asymmetric and symmetric O−D stretching and the symmetric, scissoring, O−D deformation. For a free D_2O molecule in a vacuum these modes appear at 2789, 2666, and 1179 cm^{-1}, respectively.[25] However, upon interaction with other D_2O molecules, e.g., in liquid water or ice, the vibrational modes are heavily affected by hydrogen bond interactions, and they shift to lower frequencies and appear as broad features. Bulk D_2O absorbs in two regions. One peak appears around 1200 cm^{-1} and another one in the 2250−2750 cm^{-1} region. This latter peak contains features that can be used to extract information about the phase behavior and surface chemistry of the ice overlayers, and these topics have been thoroughly discussed in the literature.[19,20,24,26−31] In a perfect crystal of hexagonal D_2O ice, for example, each molecule forms hydrogen bonds with four other molecules. This tetragonal symmetry is broken at the surface of a crystal or at imperfections resulting in a reduction of the coordination number and the appearance of new vibrations, so-called surface modes. Four surface modes have been observed of which three are relatively easy to locate at ∼2725−2740 cm^{-1} (free O−D stretching), ∼2640 cm^{-1} (free O orbital lobe), and ∼2580 cm^{-1} (four coordinated, distorted D_2O), respectively.[32] Moreover, previous reports show that small clusters of D_2O ice (2−10 molecules per cluster) display a similar set of narrow surface modes.[33,34] It is also observed that small clusters with a large surface-to-volume ratio tend to shift the surface modes toward high frequencies.[33,35,36] The exact frequencies of such surface modes can also be tuned by coating the ice cluster with molecules[28,31] or by depositing ultrathin ice overlayers onto chemically modified surfaces, e.g., on surfaces of varying wettability properties.[19] Thus, it can be concluded that surface modes appear at higher frequencies as compared to those observed for fully four-coordinated hexagonal (I_h) D_2O ice, and as a rule of thumb, D_2O ice modes appearing above 2520 cm^{-1} are attributed to surface modes and those below 2520 cm^{-1} belong to bulk (3D) modes.[32,37]

The serine thiol, Scheme 1, was used as a reference molecule in our experiment, since the molecule has the same backbone as the phosphate derivative. The molecule has been shown to form high-quality monolayers on gold with a thickness of 9 Å, approximately half of the thickness of a monolayer of phosphate analogue, 18 Å. This large difference in thickness is due to the bulkiness of the phosphate group.[9] The contact angles with water for the serine and serinephosphate SAMs are 26 and <10°, respectively. The phosphate can exist as a charged or a neutral group, as well as a mixture thereof, on the SAM surface, depending on the nature of solvents and buffers used. We therefore equilibrated the serinephosphate SAMs prior to D_2O deposition in solutions containing an excess of counterions H^+, Na^+, and Ca^{2+}. The different counterions affect the appearance of the RA spectra mainly in the phosphate (P−O) stretching region, and these interactions have been discussed before.[9]

The D_2O molecules are deposited onto the substrate surface at ∼85 K, a temperature that severely limits the lateral mobility. Thus, the D_2O molecules are assumed to stick to the substrate at the point where they hit the surface. The structure of the D_2O ice layer at low coverage is therefore mainly affected by interaction with the SAM surface. Upon increasing the surface coverage, the probability for a D_2O molecule to adsorb at an empty site on the substrate decreases while the probability of D_2O adsorbing on top of other D_2O molecules already residing to the surface increases. This gives a hint that the main effects on the D_2O ice overlayer will occur in the submonolayer regime. However, earlier studies suggest that the effect of the surface may extend into several adlayers of D_2O, depending on the nature and strength of the D_2O−surface interaction.[18,24]

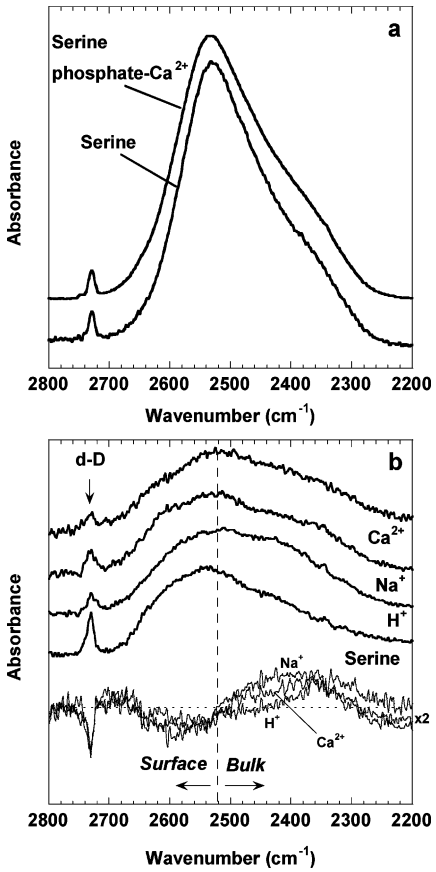

Figure 1. RA spectra of (a) ~2.5 monolayers D_2O adsorbed to the serine analogue surface and to the serinephosphate analogue surface with Ca^{2+} as a counterion (b) ~0.2 monolayers D_2O adsorbed to the serine analogue surface and serinephosphate with H^+, Na^+, and Ca^{2+} as a counterion, respectively. For clarity, the difference spectra, where the spectrum has been subtracted from the H^+, Na^+, and Ca^{2+} spectra are also displayed. The *d*−*D* (free O−D stretch) peak is marked as well as the approximate boundary between surface and bulk modes (---); see text for details.

In this study are the RA spectra for thick D_2O overlayers (>2 monolayers) close to independent of the nature of surfaces, cf. the RA spectra obtained for ~2.5 monolayers of D_2O ice on the serine and serinephosphate−Ca^{2+} SAMs, Figure 1a. A comparison with previous modeling of RA spectra suggests that amorphous-like ice is formed.[21] At low D_2O coverage (less than a full monolayer), however, there is a clear difference in the D_2O ice structure on the serine and serinephosphate surfaces. Figure 1b displays the RA spectra of ~0.2 monolayers (~0.8 Å) D_2O deposited onto the four different surfaces at 85 K. The difference is especially pronounced when comparing the spectra of serine and serinephosphate, whereas the difference is less pronounced when comparing the spectra of the serinephosphate with different counterions. The RA spectra of D_2O deposited onto the serinephosphate surfaces display relatively less intense surface modes than D_2O deposited onto serine. This is clearly displayed in the spectra as an overall increase in the intensity below 2520 cm^{-1} and a decrease in the intensity above 2520 cm^{-1}, where the decrease of the non-hydrogen-bonded O−D vibration at 2738 cm^{-1} is particularly apparent; see also the difference spectra (lower panel) in Figure 1b. The difference is probably due to the presence of the highly polar phosphate entity that possesses both hydrogen bond donating and accepting groups. These groups can readily replace the missing hydrogen bonds in the ice overlayer, resulting in an enhanced intensity of the bulk D_2O modes (below 2520 cm^{-1}) and a reduced

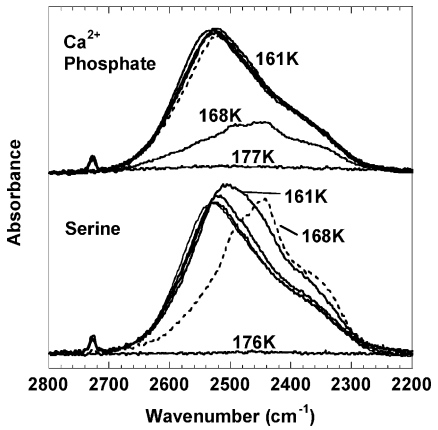

Figure 2. Dynamic IRAS of ~2.5 monolayers D_2O adsorbed to the Ca^{2+} serine phosphate analogue (top) and serine analogue substrate (bottom). Each spectrum is averaged over a 7 K temperature span, since the surface temperature increases linearly during measurement.

intensity of the vibrations originating from noncoordinated D_2O bonds (surface modes). In the case of D_2O being deposited to the serinephosphate with Ca^{2+} as a counterion, the free O−D vibration is the weakest for the four surfaces, suggesting that also the counterion plays an important role for the coordination (hydration) of D_2O molecules to serinephosphate groups. Thus, it is from this way of reasoning plausible to assume that the D_2O ice overlayer interacts more vigorously with the serinephosphate SAMs than with the corresponding serine SAM (see below).

Desorption Dynamics. The structure of the D_2O ice overlayers may also be temperature-dependent, which can be explored with dynamic IRAS. The sampling time during dynamic IRAS is relatively short, and the signal strength of a submonolayer of D_2O is weak. This makes it difficult to monitor the structural differences for D_2O coverage of less than 1 monolayer because of high noise levels in the RA spectra. But for a D_2O coverage exceeding ~2 monolayers the *S*/*N* ratio is acceptable and allows for dynamic investigations. Figure 2 displays the dynamic RA spectra for approximately 2.5 monolayers of D_2O deposited onto the serine and serinephosphate−Ca^{2+} SAMs, respectively. When comparing these spectra to the low-coverage spectra in Figure 1b, the difference in the surface to bulk mode intensity ratios is apparent, especially the intensity of the *d*−*D* peak at ~2730 cm^{-1} compared to the main peak. As the sample temperature is increased the D_2O layer deposited onto the serine SAM changes gradually its structure from amorphous- to crystalline-like ice before it finally disappears at about 168−176 K. Worth noticing is that the shift in the spectrum toward lower frequencies is consistent with the formation of a 3D bulk ice structure, i.e., hexagonal I_h ice.[24]

Moreover, the free O−D stretching peak disappears as the amorphous ice undergoes transition to crystalline-like ice. Thus, our data suggest that the interaction with the substrate is relatively weak, allowing the ice to rearrange and form a new structure. The D_2O ice overlayer on the serinephosphate−Ca^{2+} SAM surface does not undergo the same gradual change in structure as observed for serine. The only visible change in the RA spectrum appears very late during the desorption process, i.e., when a substantial amount of the ice layer already has desorbed. The delay in the phase transition is most likely a direct consequence of the stronger interaction between the D_2O ice and the serinephosphate−Ca^{2+} surface. This interaction influences the lateral mobility of the D_2O molecules in intimate contact with the serinephosphate−Ca^{2+} and prevents indirectly the subsequent adlayers of D_2O from changing structure into

crystalline-like I_h ice. Thus, pinning to the substrate influences to a large extent the phase behavior of thin ice layers, a phenomenon that has been observed before.[21,37]

To increase the understanding of the interaction between D_2O and the SAM surfaces, TPD-MS traces were recorded in parallel to the dynamic RA spectra. The binding strength (energy of desorption) of the D_2O molecules deposited at the surface at low coverages can thereby be determined. TPD-MS can also be utilized to identify different modes of adsorption on the SAM surfaces. Figure 3a shows the MS signal for D_2O desorbing from serine and serinephosphate SAM, here with Ca^{2+} as a counterion, for D_2O coverage between 0.2 and ~11 monolayers. As the coverage increases (>1 monolayer), the peak desorption temperature increases continuously with coverage, suggesting that desorption of D_2O from both the serine and serinephosphate surfaces follows zero-order kinetics. The mass trace obtained at high coverage on both the serine and serinephosphate−Ca^{2+} displays a single broad peak most likely originating from a multitude of energetically narrow sites on the surface. At high coverage there is also a slight irregularity (shoulder) in the MS trace, a phenomenon that has been attributed to reflect the transition from amorphous- to polycrystalline-like ice.[38,39] The shoulder in the traces most likely appears because crystalline D_2O ice has a lower desorption rate than amorphous D_2O.[40] The transition from amorphous- to crystalline-like D_2O ice is also clearly visible in the dynamic RA spectra for D_2O deposited onto serine for a D_2O coverage of ~2.5 monolayers, Figure 2. This transition is barely visible in the RA spectra for lower coverage (data not shown), suggesting that the D_2O ice layers must exceed a critical thickness (~2 monolayers/6 Å) in order to adopt a structure characteristic for crystalline ice.

The largest effects on the desorption behavior are seen in the TPD-MS traces recorded at low D_2O coverage on the different SAM surfaces. The TPD-MS traces, obtained at a constant D_2O coverage of 0.2 ± 0.02 monolayer (0.8 ± 0.08 Å), are displayed in Figure 3b. As can be seen, changing the tail group and/or the counterion affects the desorption behavior of the D_2O ice overlayer to a varying degree. For example, the desorption peak temperature and shape are not very different when comparing the trace of D_2O desorbing from serinephosphate, in the form of a free base (H^+), with that obtained for serine. Moreover, each desorption trace consists of a sharp and asymmetric peak with a high-temperature tail. This tail originates partly from the limited pumping capacity of the vacuum system, which gives rise to a slight increase in the background partial pressure of D_2O in the chamber. Exchange of counterions to Na^+ or Ca^{2+} increases the desorption peak temperature as well as the width of the MS peaks. The broadening of the MS peak is especially pronounced in the case of D_2O desorbing from the serinephosphate−Ca^{2+} surface. Thus, it seems reasonable to conclude that this broad peak is due to desorption from several unresolved and narrow sites on the serinephosphate−Ca^{2+} surface. One can of course argue that the high-temperature tail in the Ca^{2+} phosphate trace is due to the limited pumping capacity of the ultrahigh-vacuum system. However, we find this explanation less likely because the high-temperature tail is far more pronounced than expected for such a low coverage. If the tail solely appears because of the limited pumping capacity of the system, then we also expect to observe a tail of similar shape in the trace obtained from the Na^+ phosphate surface (same coverage and same desorption peak temperature). This is definitely not the case. Instead we observe a symmetric desorption peak, without high-temperature tail, for the Na^+ sample, Figure 3b. Thus, we conclude that the high-temperature tail in the Ca^{2+} trace appears because of specific interaction(s) with the surface (e.g., with yet unidentified sites). One possible way to shed some light on the nature of the "unidentified" sites is to vary the temperature ramping rate. This type of experiment, however, is beyond the scope of the present contribution. Interestingly, the shape of the trace resembles that obtained for another system of strongly bound water on carboxylic acid

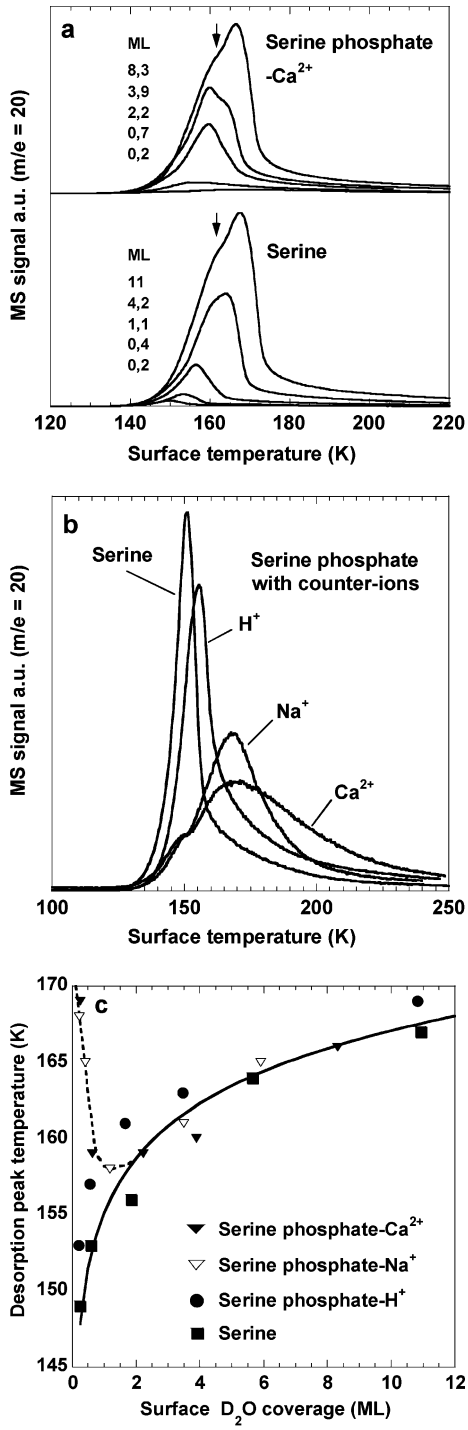

Figure 3. MS traces of (a) D_2O of different monolayer (ML in the figure) coverage desorbing from the Ca^{2+} serinephosphate analogue and serine analogue substrate. The arrow points out the irregularity originating from the amorphous to polycrystalline effect discussed in the text. (b) ~0.2 monolayer D_2O desorbing from serine and serinephosphate analogues with H^+, Na^+, and Ca^{2+} as a counterion, respectively. The Ca^{2+} and serine trace are displayed also in a. (c) MS peak temperature plotted as a function of surface coverage in monolayers. Lines are inserted as a guide to the eye.

SAMs.[22] There is in both the Na^+ and Ca^{2+} serinephosphate traces a weak shoulder at ~150 K. This peak arises from D_2O weakly bound to other D_2O molecules and not directly to the phosphate surface, and it grows in intensity with increasing D_2O coverage and becomes eventually the dominant feature of the MS trace; see Figure 3a. Figure 3c summarizes the desorption peak temperatures as a function of coverage (0−12 monolayers) for the serine and serinephosphate surfaces displayed in Figure 3a,b. The desorption peak temperature increases continuously with coverage for all surfaces at coverages above ~2 monolayers. It is also interesting to note that the peak desorption temperatures obtained for each coverage (>2 monolayers) are essentially the same (±3 K) regardless of the chemical nature of the surface. Furthermore, the peak desorption temperatures obtained for the serinephosphate−H^+ is almost identical to those observed for the serine (OH) surface for all investigated coverages. However, the desorption peak temperature of these two surfaces, at a coverage of 0.2 monolayer, differ substantially from the serinephosphate surfaces having Na^+ and Ca^{2+} as counterions. Both the Na^+ and Ca^{2+} phosphate display desorption peaks at about 170 K for a coverage of ~0.2 monolayers, a value that is ~20 K (ΔE_{des} = ~6 kJ/mol) higher than those obtained for the other two surfaces. The energy of desorption, E_{des}, is estimated by assuming a first-order desorption model at these low coverages and by setting the preexponential factor to 10^{13} s^{-1} and the heating rate β to 0.33 K/s.[41] It is also interesting to note that the obtained values of E_{des} obtained here for the Na^+ and Ca^{2+} phosphate surfaces of 45 and 46 kJ/mol, respectively, are considerably higher that those reported for analogous self-assembled monolayer systems, except for the E_{des} reported for D_2O desorbing from carboxylic acid SAM, another substrate also displaying strong hydrogen bonding properties.[22] The corresponding values for serinephosphate−H^+ and serine are 41 and 40 kJ/mol, respectively. This supports our TPD-IRAS observation that the D_2O ice layer is strongly bound to the serinephosphate surfaces with Na^+ and Ca^{2+} counterions and that this strongly bound layer influences the lateral mobility of the D_2O molecules and thereby also the phase behavior of thicker ice layers, cf. those in Figure 2. The desorption peak temperatures obtained for the Na^+ and Ca^{2+} phosphate surfaces decrease rapidly with increasing coverage and approach the desorption peak temperatures obtained for the two other surfaces in the 1−2 monolayers regime. Lateral interactions with other D_2O molecules obviously become very prominent at these coverages. Although the D_2O−D_2O interactions are weaker than the D_2O−phosphate interactions, they tend to dominate and become the main part of the MS signal at a coverage of ~2 monolayers, after which the MS traces of D_2O desorbing from phosphate (H^+, Na^+, and Ca^{2+}) and serine behave similarly.

Conclusions

We have studied the interaction and phase behavior of D_2O ice overlayers (0.2−11 monolayers) onto a number of model phosphate surfaces using infrared spectroscopy and mass spectrometry. These surfaces are, as a zero-order model, aimed at mimicking the properties of bone mineral, i.e., hydroxyapatite. Self-assembled monolayers with serine and serinephosphate tail groups with three different counterions H^+, Na^+, and Ca^{2+} have been prepared on gold. The serinephosphate SAMs with Na^+ and Ca^{2+} as a counterion behave qualitatively the same for ice coverage/film thickness ranging from 0.2 to 11 monolayers (0−40 Å). Ultrathin D_2O ice overlayers (~0.2 monolayer) are strongly bound to these surfaces, possibly at several energetically narrow sites, and the energy of desorption is generally higher than previously published values obtained for analogous high-energy SAMs. Ultrathin D_2O ice deposited onto serine and serine phosphate with H^+ as a counterion is less strongly bound to the SAM surface. These differences in interaction energy also influence the lateral mobility of D_2O molecules, a behavior that is clearly visible in dynamic infrared studies of the phase properties of thick D_2O ice overlayers (~2.5 monolayers). For example, the D_2O ice overlayer on the serine surface undergoes a gradual change from amorphous to crystalline-like ice over a fairly broad range of temperatures, whereas the same transition occurs abruptly at high temperatures on the serine phosphate SAMs with Na^+ and Ca^{2+} counterions. We believe that this type of fundamental studies of interfacial water and ice may contribute to an improved understanding of chemistry and growth of biomineral surfaces, e.g. hydroxyapatite, and in the long run to the design and development of novel implantable biomaterials.

Acknowledgment. This work was supported by the Swedish Research Council (VR) and the Swedish Foundation for Strategic Research (SSF) through the Biomimetic Materials Science Program.

References and Notes

(1) Walsh, D.; Mann, S. *Chem. Mater.* **1996**, *8*, 1944.
(2) Sarda, S.; Heughebaert, M.; Lebugle, A. *Chem. Mater.* **1999**, *11*, 2722.
(3) Saeri, M. R.; Afshar, A.; Ghorbani, M.; Ehsani, N.; Sorrell, C. C. *Mater. Lett.* **2003**, *57*, 4064.
(4) Liu, J. W.; Lu, Y. *J. Am. Chem. Soc.* **2003**, *125*, 6642.
(5) Flade, K.; Lau, C.; Mertig, M.; Pompe, W. *Chem. Mater.* **2001**, *13*, 3596.
(6) Falini, G.; Fermani, S.; Gazzano, M.; Ripamonti, A. *Chem.−Eur. J.* **1998**, *4*, 1048.
(7) Yamashita, K.; Oikawa, N.; Umegaki, T. *Chem. Mater.* **1996**, *8*, 2697.
(8) Kuther, J.; Nelles, G.; Seshadri, R.; Schaub, M.; Butt, H. J.; Tremel, W. *Chem.−Eur. J.* **1998**, *4*, 1834.
(9) Ekeroth, J.; Borgh, A.; Konradsson, P.; Liedberg, B. *J. Colloid Interface Sci.* **2002**, *254*, 322.
(10) Ekeroth, J.; Bjorefors, F.; Borgh, A.; Lundstrom, I.; Liedberg, B.; Konradsson, P. *Anal. Chem.* **2001**, *73*, 4463.
(11) Ekeroth, J.; Konradsson, P.; Bjorefors, F.; Lundstrom, I.; Liedberg, B. *Anal. Chem.* **2002**, *74*, 1979.
(12) Israelachvili, J.; Wennerström, H. *Nature* **1996**, *379*, 219.
(13) Kasemo, B. *Surf. Sci.* **2002**, *500*, 656.
(14) Vogler, E. A. *J. Biomater. Sci., Polym. Ed.* **1999**, *10*, 1015.
(15) Brown, G. E. *Science* **2001**, *294*, 67.
(16) Neuman, W. F.; Neuman, M. W. *Chem. Rev.* **1953**, *53*, 1.
(17) Sukhodub, L. F.; Moseke, C.; Sukhodub, L. B.; Sulkio-Cleff, B.; Maleev, V. Y.; Semenov, M. A.; Bereznyak, E. G.; Bolbukh, T. V. *J. Mol. Struct.* **2004**, *704*, 53.
(18) Engquist, I.; Lestelius, M.; Liedberg, B. *Langmuir* **1997**, *13*, 4003.
(19) Engquist, I.; Liedberg, B. *J. Phys. Chem.* **1996**, *100*, 20089.
(20) Engquist, I.; Lundstrom, I.; Liedberg, B. *J. Phys. Chem.* **1995**, *99*, 12257.
(21) Engquist, I.; Lundstrom, I.; Liedberg, B.; Parikh, A. N.; Allara, D. L. *J. Chem. Phys.* **1997**, *106*, 3038.
(22) Dubois, L. H.; Zegarski, B. R.; Nuzzo, R. G. *J. Am. Chem. Soc.* **1990**, *112*, 570.
(23) Trakhtenberg, S.; Naaman, R.; Cohen, S. R.; Benjamin, I. *J. Phys. Chem.* **1997**, *101*, 5172.
(24) Nuzzo, R. G.; Zegarski, B. P.; Korenic, E. M.; Dubois, L. H. *J. Phys. Chem.* **1992**, *96*, 1355.
(25) Herzberg, G. *Infrared and Raman Spectra of Polyatomic Molecules*; van Nostrand: Princeton, NJ, 1945.
(26) Scatena, L. F.; Brown, M. G.; Richmond, G. L. *Science* **2001**, *292*, 908.
(27) Hernandez, J.; Uras, N.; Devlin, J. P. *J. Phys. Chem. B* **1998**, *102*, 4526.
(28) Rowland, B.; Kadagathur, N. S.; Devlin, J. P.; Buch, V.; Feldman, T.; Wojcik, M. J. *J. Chem. Phys.* **1995**, *102*, 8328.
(29) Devlin, J. P.; Sadlej, J.; Buch, V. *J. Phys. Chem. A* **2001**, *105*, 974.

(30) Devlin, J. P.; Joyce, C.; Buch, V. *J. Phys. Chem. A* **2000**, *104*, 1974.

(31) Delzeit, L.; Devlin, J. P.; Buch, V. *J. Chem. Phys.* **1997**, *107*, 3726.

(32) Devlin, J. P.; Buch, V. *J. Phys. Chem.* **1995**, *99*, 16534.

(33) Paul, J. B.; Provencal, R. A.; Chapo, C.; Petterson, A.; Saykally, R. J. *J. Chem. Phys.* **1998**, *109*, 10201.

(34) Paul, J. B.; Collier, C. P.; Saykally, R. J.; Scherer, J. J.; OKeefe, A. *J. Phys. Chem. A* **1997**, *101*, 5211.

(35) Nauta, K.; Miller, R. E. *Science* **2000**, *287*, 293.

(36) Huisken, F.; Kaloudis, M.; Kulcke, A. *J. Chem. Phys.* **1996**, *104*, 17.

(37) Engquist, I. *Microscopic Wetting: Structural and Morphological Studies of Thin Ice on Self-Assembled Monolayers*; Linköping University: Linköping, Sweden, 1996.

(38) Smith, R. S.; Huang, C.; Wong, E. K. L.; Kay, B. D. *Phys. Rev. Lett.* **1997**, *79*, 909.

(39) Dohnálek, Z.; Ciolli, R. L.; Kimmel, G. A.; Stevenson, K. P.; Smith, R. S.; Kay, B. D. *J. Chem. Phys.* **1999**, *110*, 5489.

(40) Speedy, R. J.; Debenedetti, P. G.; Smith, R. S.; Huang, C.; Kay, B. D. *J. Chem. Phys.* **1996**, *105*, 240.

(41) Redhead, P. A. *Vacuum* **1962**, *12*, 203-211.